Delft University of Technology

An improved semi-analytical method for 3D slope reliability assessments

Varkey, Divya; Hicks, Michael; Vardon, Phil

Important note
To cite this publication, please use the final published version (if applicable).
Please check the document version above.

Research Paper

An improved semi-analytical method for 3D slope reliability assessments

D. Varkey, M.A. Hicks*, P.J. Vardon

Section of Geo-Engineering, Faculty of Civil Engineering and Geosciences, Delft University of Technology, the Netherlands

ARTICLE INFO

ABSTRACT

An improved semi-analytical method for calculating the reliability of 3D slopes with spatially varying shear strength parameters is proposed. The response of an existing semi-analytical method has been compared with that of the computationally more intensive, but more general, random finite element method (RFEM), demonstrating that the simpler method underestimates the failure probability. An alternative relationship for the expected failure length and two correction factors are proposed, which modify the original formulation of the simpler method. The proposed approach gives substantially improved results that compare favourably with those obtained by RFEM, and therefore provides a more accurate simplified solution.

1. Introduction

Calculating the stability of slopes began centuries ago, starting with various analytical methods and gradually progressing towards numerical simulations. However, a complicating factor is the inherent nature of soil to be spatially variable [1] due to a combination of various geological, environmental and physico-chemical processes, among others. The quantification of spatial variability (or heterogeneity) is not a trivial task and requires extensive field and laboratory tests [2,3]. Hence, the stability of slopes is conventionally calculated deterministically, i.e., by considering the entire slope to be made up of one or more homogeneous layers and by ignoring the spatial variability of soil properties within the layers. The outcome of such an analysis is a single value of the factor of safety (FS), which reveals nothing about the reliability of, or risks associated with, that slope. However, the presence of heterogeneity influences the slope stability, as well as the location and type of failure mechanism [4,5], and ignoring it has been shown to have a significant influence on computations of geotechnical performance [6–9].

Reliability-based analysis methods have been developing since the early 1970s to account for the uncertainties associated with a project, including those associated with soil heterogeneity. These include the first order second moment method [10], the first order reliability method [11,12], the point estimate method [13], the stochastic response surface method [14,15] and the random finite element method (RFEM) [16]. In particular, RFEM has proven to be an effective and versatile method [6,17], in which multiple possible responses of the structure are computed. Lloret-Cabot et al. [18] and Li et al. [19] have proposed ways to efficiently use available field data to condition these

responses in order to improve confidence through reducing uncertainty.

Much research has been done in 2D slope reliability analysis to understand the influence of various levels of anisotropy of the heterogeneity in the mechanical and hydraulic parameters [20], and in making use of inverse analysis techniques to reduce the uncertainty in hydraulic conductivity by using pore pressure measurements [21]. These studies are based on the simplifying assumption that the mechanical and hydraulic parameters are correlated over an infinite distance in the third dimension. However, this is not the case, which indicates a need for 3D reliability analysis.

So far, only a limited amount of research has been done in 3D, due (at least in part) to the large computational requirements. This is especially true for RFEM, which does not make any prior assumptions regarding the location and shape of the failure mechanism, and hence requires large computational time and memory to carry out multiple finite element analyses. Spencer and Hicks [22] and Hicks and Spencer [4] used 3D RFEM to investigate the influences of anisotropy of the heterogeneity in the undrained shear strength and slope length in the third dimension on the estimation of the failure probability. They also grouped the failure modes into three categories, which were based on the horizontal scale of fluctuation of the shear strength relative to the slope dimensions. Meanwhile, Hicks et al. [5,23] and Huang et al. [24] developed strategies to quantify the failure consequences in terms of slide volume by using a threshold crossing technique linked to the out-of-face displacements and the K-means clustering method, respectively.

Vanmarcke [25,26] pioneered 3D reliability assessments of slopes by making certain (important) simplifying assumptions, and thereby developed a simplified method which gives a quick and convenient solution. Li et al. [27] and Varkey et al. [28] compared the performance

---

* Corresponding author.
E-mail address: m.a.hicks@tudelft.nl (M.A. Hicks).

of this method with that of RFEM for reliability predictions of an idealised 3D slope, for cohesive and c–ϕ soils, respectively, and have highlighted those instances in which the two methods give similar results, as well as those in which there are significant differences. Moreover, Hicks and Li [29] investigated slope length dependency for cohesive soils by comparing 3D RFEM with the Vanmarcke [25] method and the "2.5D" method of Calle [30].

This paper further investigates the differences in 3D solutions obtained by RFEM and Vanmarcke's method for a slope with a fixed length in the third dimension and, having established the differences to be due to simplifying assumptions in Vanmarcke's method, investigates an approach to improve its performance. Uncertainty in the spatial variability of the shear strength parameters (c and ϕ) is the focus of the paper. The authors use random fields of shear strength parameters in modifying Vanmarcke's method, so that it gives satisfactory results over the full range of possible levels of anisotropy of the heterogeneity in shear strength while retaining the simplicity of the solution. Specifically, an alternative relationship for the expected failure length and some modifications, quantified in terms of correction factors, are proposed for the original Vanmarcke method. Curves have been plotted for calibrating the correction factors and recommended values for them are also provided. These curves have been validated for a range of slope heights and slope angles.

2. Random finite element method

RFEM is based on a Monte Carlo simulation and links random field theory, for modelling the spatial variability of soil property values, with finite elements, for computing structure response.

In this paper, independent (i.e. uncorrelated) random fields for both shear strength variables have been generated using local average subdivision (LAS) [31], which requires only the mean (μ), standard deviation (σ) and scales of fluctuation (i.e. spatial correlation distances) in the three dimensions , where θ_z is the vertical scale of fluctuation (θ_v) and $\theta_x = \theta_y$ are the horizontal scales of fluctuation (θ_h). The random fields are here generated using the Markov covariance function:

$$\beta_M\left(\tau_x,\ \tau_y,\ \tau_z\right) = \sigma^2 \exp\left(-\frac{2\tau_z}{\theta_z} - \sqrt{\left(\frac{2\tau_x}{\theta_x}\right)^2 + \left(\frac{2\tau_y}{\theta_y}\right)^2}\right) \tag{1}$$

where τ_x, τ_y and τ_z are the lag distances in the respective directions. An isotropic random field is initially generated using $\theta = \theta_x = \theta_y = \theta_z$ in Eq. (1), and this field is then post-processed by squashing and/or stretching in the respective directions to generate the required level of anisotropy ($\xi = \theta_h/\theta_v$); see Hicks and Samy [6,17] and Hicks and Spencer [4] for details.

Following the random field generation, the field values are mapped to the Gauss points of a finite element mesh, and the boundary value problem is analysed by finite elements. In this paper, the strength reduction method is used to determine the factor of safety of the slope in each realisation, and multiple realisations are performed to generate a distribution of safety factors.

Hicks and Spencer [4] conducted similar 3D RFEM analyses for a cohesive slope with θ_v equal to one fifth of the slope height, and proposed three categories of failure mode, for different values of θ_h with respect to the slope height (H) and slope length (L):

(i) Mode 1 ($\theta_h < H$): Failure propagates through weak and strong zones alike, resulting in considerable averaging of property values along the entire slope length. This is similar to a 2D analysis based on the mean property values.
(ii) Mode 2 ($H < \theta_h < L/2$): Failure propagates through semi-continuous weaker zones, resulting in discrete 3D failures and a wide range of possible solutions.
(iii) Mode 3 ($\theta_h > L/2$): Failure propagates through weak zones and

there is a wider range of possible solutions. The failure impacts the entire slope length, and the solution is analogous to that for a 2D stochastic analysis.

Hicks et al. [5] investigated the modes of failure in more detail, by automatically computing failure geometries in 3D RFEM. It was thereby shown that the Mode 2 category of failure is widespread, and may also occur for the relatively small and large values of θ_h normally associated with failure mode categories Mode 1 and Mode 3.

3. Vanmarcke's method

Vanmarcke [25] considered 3D slope reliability by extending a circular slip circle to a cylindrical failure surface with resisting end-sections within a probabilistic framework. The load (due to self weight) and cross-sectional characteristics were assumed to be constant along the slope axis. Hence, only the uncertainty due to the natural variability of the soil strength mobilised along the failure surface was considered. Vanmarcke [25] first considered the spatial variability in undrained shear strength, and later considered a slope with spatial variability in drained soil shear strength along with several other extensions [26].

The general method predicts the failure length b, along the embankment axis, which maximises the probability of failure occurring when centred at a specific location (see Fig. 1). Using the classical circular-arc stability approach, the factor of safety of the slope is given by

$$F_b = \frac{(s_b L_a b)r + R_e}{(Wb)a} \tag{2}$$

$$R_e = (2s_e A)r' \tag{3}$$

where s_b is the averaged shear strength along the failure surface of length b, L_a is the length of the cross-sectional failure arc, r is the lever arm of the resisting moment about the centre of rotation, R_e is the resisting moment of the end-sections defined by Eq. (3), W is the weight per unit length of the sliding mass, a is the lever arm of the centre of gravity of the sliding mass about the same centre of rotation, s_e is the shear strength over the two end-sections, A is the area of each end-section and r' is the effective rotation arm for the end sections.

For a spatially variable shear strength, and by assuming a deterministic overturning moment and neglecting any variance in the end-resistance, the mean and standard deviation (denoted by a bar and tilde, respectively, above the random variable) of the factor of safety are given by

$$\overline{F_b} = \frac{(\overline{s_b} L_a b)r + (2\overline{s_e} A)r'}{(Wb)a} \tag{4}$$
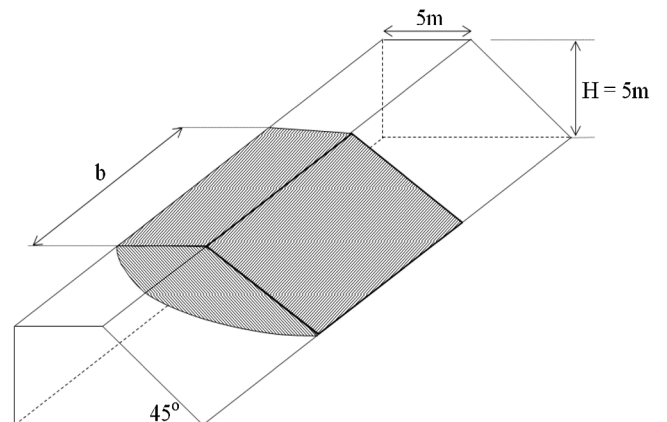

Fig. 1. Failure mass within a 3D slope (based on [25]).

$$\widetilde{F_b} = \frac{(\widetilde{s_b} L_a b) r}{(Wb) a} \tag{5}$$

For a stationary random field of the shear strength parameters, the averaged shear strength on the end-sections ($\overline{s_e}$) and the averaged shear strength along the failure surface ($\overline{s_b}$) are assumed to be equal to the mean of all point shear strength values ($\bar{s}$) throughout the slope [25]. Following Vanmarcke [25] and assuming $r' = r$, Eq. (4) simplifies to

$$\overline{F_b} = \frac{(\bar{s} L_a) r}{Wa} \left[1 + \frac{d}{b} \right] \tag{6}$$

and thereby to

$$\overline{F_b} = \overline{F} \left[1 + \frac{d}{b} \right] \tag{7}$$

where $\overline{F}$ is the mean plane strain factor of safety, which can be calculated via any appropriate method, and d is the effective width of the end-sections given by

$$d = 2A/L_a \tag{8}$$

The random shear strength at any point, as well as the mean and variance of all point shear strength values, are respectively given by [26]

$$s = c + \sigma_n \tan(\phi) \tag{9}$$

$$\bar{s} = \bar{c} + \overline{\sigma_n} \tan(\bar{\phi}) \tag{10}$$

$$\widetilde{s}^2 = \widetilde{c}^2 + \overline{\sigma_n}^2 (\tan(\widetilde{\phi}))^2 \tag{11}$$

where c is the cohesion, ϕ is the friction angle and σ_n is the stress normal to the failure surface.

Assuming that the failure surface is known, the averaged value of shear strength over the failure length (s_b) is calculated as the average of spatial averages of strength over the failure surface for embankment segments of unit length (s_1) perpendicular to the cross-section. The greater the length of the failure arc for an embankment segment of unit width, over which the point shear strength values are averaged, the more the fluctuations in shear strength cancel each other out, resulting in a reduction in the standard deviation. Moreover, the greater the length of the cylindrical surface along the embankment axis, over which s_1 is averaged, the more the fluctuations in s_1 cancel each other out, resulting in a further reduction in the standard deviation. Hence, Eq. (5) may be expressed as

$$\widetilde{F_b} = \frac{\Gamma(L_a) \Gamma(b) (\widetilde{s} L_a b) r}{(Wb) a}$$

$$\widetilde{F_b} = \Gamma(L_a) \Gamma(b) V_s \overline{F} \tag{12}$$

where V_s is the coefficient of variation of the point shear strength ($= \widetilde{s}/\bar{s}$), and $\Gamma(L_a)$ and $\Gamma(b)$ are the reduction factors relating to the standard deviation along the failure arc and failure length, respectively. $\Gamma(b)$ is given by

$$\Gamma(b) = \sqrt{(\theta_h/b)}; \quad \theta_h < b$$
$$\Gamma(b) = 1; \quad \theta_h \geqslant b \tag{13}$$

and $\Gamma(L_a)$ is obtained by replacing b with L_a and θ_h with the equivalent scale of fluctuation (based on both θ_h and θ_v) along the failure arc (for details, see [25]).

Both $\overline{F_b}$ and $\widetilde{F_b}$ are dependent on the failure length (b). When the probability of failure is considered for a length centred at a specific location, there is a critical length (b_c) which maximises the probability of failure occurring at that location. Vanmarcke [25] proposed the following equation for the expected failure length:

$$b = b_c = \frac{\overline{F}}{\overline{F} - 1} d; \quad b_c > \theta_h$$
$$b = \theta_h; \quad b_c \leqslant \theta_h \tag{14}$$

4. Comparison of Vanmarcke and RFEM solutions

A 50 m long slope, with the geometry shown in Fig. 1, has been analysed by Vanmarcke's method and RFEM. The finite element model was meshed by 4000, 20-node hexahedral elements, which were 0.5 m deep and 1 m × 1 m in plan (except along the slope face), and used 2 × 2 × 2 Gaussian integration. The mesh was fixed at the base, with rollers on the back face preventing movement perpendicular to the face, and rollers on the two end-faces allowing movement only in the vertical direction. The end-faces were fixed against horizontal movements because Spencer [32] found that allowing horizontal movement on the end-faces appeared to result in a bias of failures congregating towards the ends of the slope; this was thought to be due to the implied symmetry of the random field about the mesh end boundaries. A further investigation and explanation of the boundary conditions is given in Hicks and Li [29].

In each realisation of the RFEM analysis, an independent random field was generated for each shear strength parameter. The parameter values were then assigned to the finite element mesh at the Gauss point level, and the finite element analysis carried out using the strength reduction method. Gravity loading was applied to the model to generate the in situ stresses, and the resulting shear stresses at the integration points were checked against the Mohr–Coulomb failure criterion. If the stresses exceeded the failure criterion, the excess stresses were iteratively redistributed throughout the model. If equilibrium could not be achieved within 500 iterations the analysis was deemed to have reached failure; otherwise, the shear strength parameters were reduced in the subsequent step and the whole process repeated until failure occurred. The lowest factor by which the shear strength parameters needed to be reduced to induce failure was taken to be the safety factor for that realisation.

The soil parameter values are listed in Table 1, and a normal distribution was considered appropriate for both c and ϕ. Note that the coefficients of variation ($=$ SD/mean) of cohesion and friction angle were set at 0.2, which is well within the typical range reported in Cherubini [33] and small enough to avoid the possibility of negative values with the normal distribution. The vertical scale of fluctuation was taken to be 1 m for all analyses (see [3] for typical values), whereas a wide range of θ_h was considered.

Based on the mean values of the shear strength parameters listed in Table 1, the plane strain factor of safety was found to be 1.4, with failure involving an $A = 12$ m^2 block of soil (per unit length) sliding along an approximately circular arc of length $L_a = 9.3$ m, giving a value of d of 2.58 m. The failure geometry was determined using finite elements and the ridge finding procedure described in Hicks et al. [5]. These derived parameters were used to compute Vanmarcke's solution (Eqs. (7) and (12)) for the same problem. Meanwhile, a total of 500 Monte Carlo realisations were carried out to make predictions using RFEM.

Fig. 2 compares the mean and standard deviation of the factor of safety for the two methods, for different values of θ_h. The mean and standard deviation of F_b (i.e., in Vanmarcke's solution) are largely dependent on the predicted failure length b, as seen in Eqs. (7) and (12).

Fig. 3 compares the mean failure length obtained by the two methods (see [28] for a comparison of slide volumes). For each RFEM

Table 1
Table of parameter values.

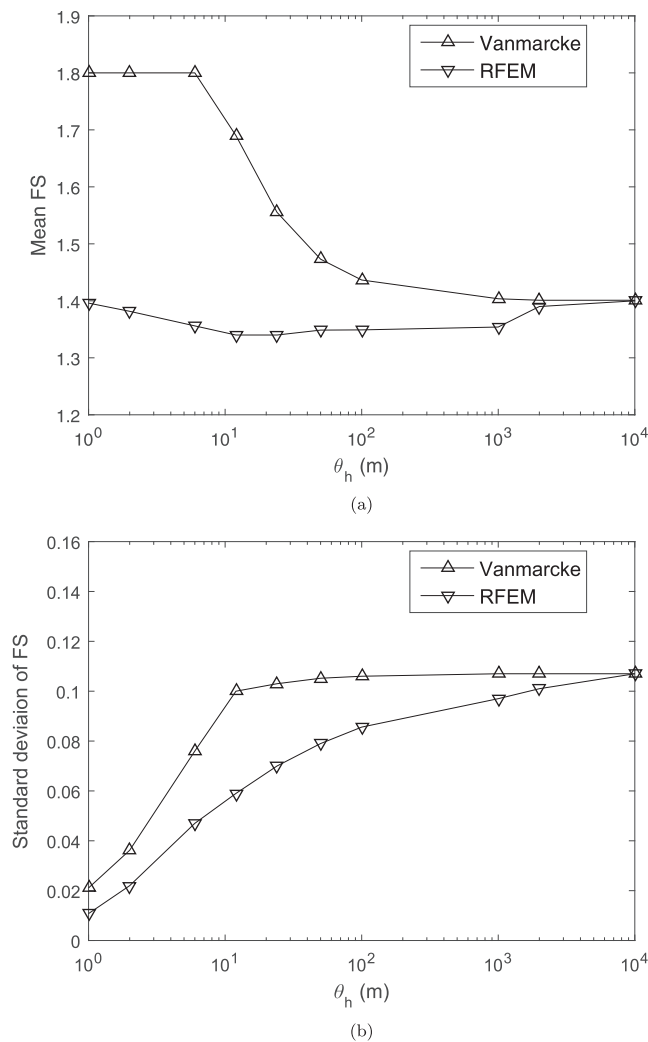| Parameter	Mean	SD	θ_v	θ_h
Cohesion, c	10 kPa	2 kPa	1 m	1 to 10^4 m
Friction angle, ϕ	25°	5°	1 m	1 to 10^4 m
Dilation angle, ψ	0°	–	–	–
Young's modulus, E	1×10^5 kPa	–	–	–
Poisson's ratio, ν	0.3	–	–	–
Unit weight, γ	20 kN/m^3	–	–	–

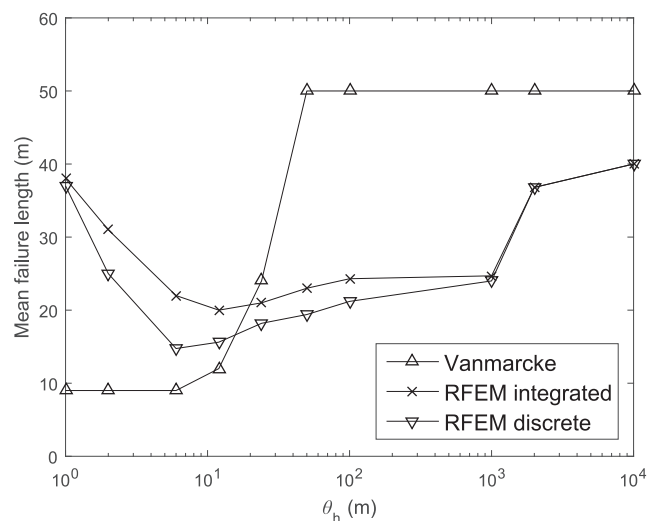Fig. 2. Comparison of (a) mean and (b) standard deviation of 3D factor of safety (FS) by the two methods.

Fig. 3. Comparison of mean failure length by the two methods.

realisation, the integrated failure length was calculated from the total number of elements in the row directly above the slope toe in which the out-of-face displacement was greater than a calibrated threshold value (representing failure), and follows the procedure described in detail in

Hicks et al. [5]. Also for each realisation, the discrete failure lengths were calculated from the number of continuously linked elements in the row directly above the slope toe in which the out-of-face displacements were greater than the same threshold value (as described in [29]). For this investigation, the threshold displacement was calibrated to be 37% of the maximum computed out-of-face displacement. The mean integrated failure length and the mean discrete failure length in the RFEM analyses were obtained by averaging over all the realisations for each θ_h. Note that although the integrated and discrete failure lengths are approximately equal at very small and very large θ_h, at intermediate values of θ_h the two differ, due mostly to the increased probability of multiple failures of shorter length relative to the slope length. Since the integrated failure length is more closely related to the slope length, discrete failure lengths are considered in the remaining part of this paper as a more independent measure of the failure length. Overall, Fig. 3 shows that the RFEM solutions are consistent with the 3 categories of failure mode identified previously by Hicks and Spencer [4]; i.e., an overriding disposition to shorter discrete 3D failures (Mode 2), but with an increased likelihood of long failures (Modes 1 and 3) at very small and very large θ_h. In contrast, the Vanmarcke solution predicts a small failure length for very small θ_h. For larger θ_h, the predicted failure length by Vanmarcke's method is equal to θ_h (Eq. (14)), but is here limited to a maximum of 50 m due to the finite length of the slope in this study.

The large difference between the mean FS of the two solutions at small θ_h is mainly due to the differences in predicted failure length, coupled with an exaggerated influence of the cylinder ends in Vanmarcke's method. At small θ_h there is considerable averaging of properties, resulting in a longer failure length in the RFEM analysis; however, Vanmarcke's method predicts short failure lengths, which results in a relatively larger contribution from the end-resistance and thereby bigger factors of safety relative to RFEM. In contrast, at very large θ_h, the two methods converge to the same FS as the 2D solution. For intermediate values of θ_h, an additional cause of the higher FS in the Vanmarcke solution is that it takes no account of failure being attracted to weaker zones; i.e., the solution is driven by the means of the property distributions.

Finally, Fig. 2 shows that convergence to a 2D solution at high θ_h is slower with two random variables compared to the similar investigation involving variability in only undrained shear strength (one random variable) in Li et al. [27]. Note that for very large θ_h, the failure length computed by RFEM is limited to the finite length of slope considered. Also, Fig. 3 shows that failure lengths computed by RFEM for very small and very large θ_h are shorter than the slope length. This is attributed to the failed zone not reaching the ends of the mesh, due to the boundary conditions which have a greater influence due to the non-zero friction angle.

5. Corrections to Vanmarcke's method

This section further investigates the reasons behind the differences in results by the two methods and proposes a way to correct for them. Firstly, three causes for the differences are evaluated as follows:

5.1. End-resistance due to geometric assumptions

The 3D cylindrical slip surface in Vanmarcke's method includes an additional resistance from both ends of the cylinder. However, this end-resistance is overestimated, as demonstrated by Li et al. [27] and reinforced by Fig. 2(a). The reason for the overestimation is partly the shape effect, as illustrated in Fig. 4. Vanmarcke assumes vertical end-sections, whereas the failure obtained in a typical RFEM analysis has a very different geometry. Moreover, Eq. (8) further overestimates the resisting moment by taking $r' \approx r$.

To correct for the overestimation in the end-resistance due to the geometric assumptions, finite element analyses were carried out for
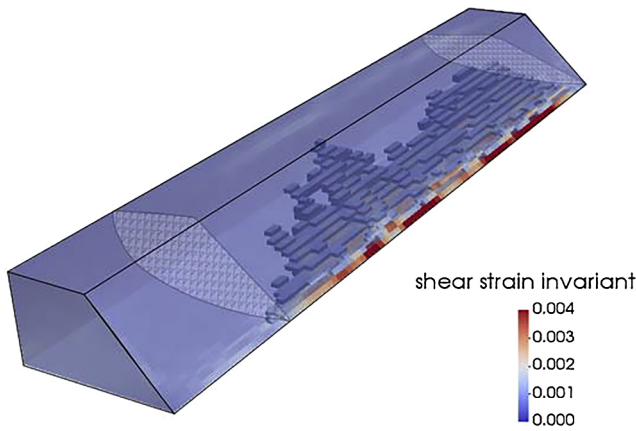
Fig. 4. RFEM realisation illustrating iso-surfaces of shear strain invariant at failure within slope, superimposed on Vanmarcke's 3D cylindrical model.
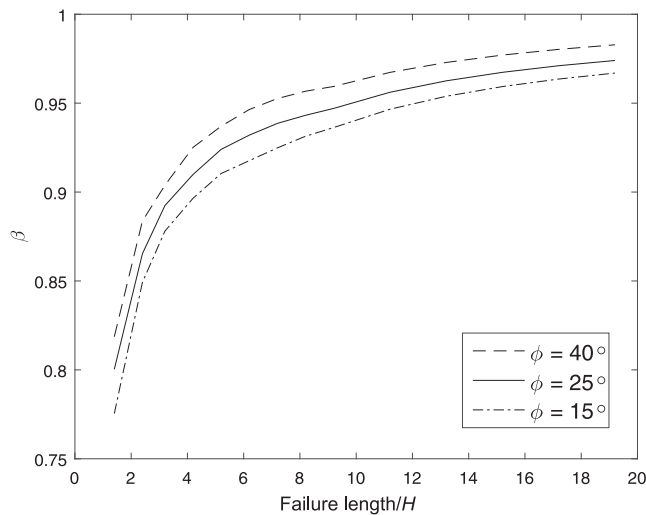

Fig. 5. Calibrated values of end-resistance correction factor (β).

Fig. 6. RFEM result for a typical realisation showing failure centred at a critical position: (a) variation in average cross-sectional strength per unit length; (b) failure mechanism.

different slope lengths based only on the mean shear strength parameters. The ratio of the factors of safety obtained by finite elements using the strength reduction method and by Vanmarcke's method, for the same failure length, is denoted as β and used here as a correction factor to account for the overestimation of end-resistance in the Vanmarcke method. Thus, the mean factor of safety $\overline{F_b}$ in Eq. (7) becomes

$$\overline{F_b} = \overline{F}\left[1 + \frac{d}{b}\right]\beta \tag{15}$$

The end-resistance correction factor (β) values calibrated for a slope with the cross-sectional geometry shown in Fig. 1 are plotted in Fig. 5 with respect to failure length, for the set of parameters listed in Table 1 and for cases representing high and low friction angles. As expected, the impact of the geometric assumptions in Vanmarcke's method reduces as the length of the failure increases. The value of β varies from 0.8 for short failures to 0.98 for very long failures, for the range of scenarios considered.

5.2. Averaged strength along slip surface

Eq. (7) is based on the assumption that the averaged mean shear strength over the failure surface ($\overline{s_b}$) is the same as the mean point shear strength ($\bar{s}$) throughout the slope. However, RFEM results indicate that weak zones have a greater influence on the failure mechanism than strong zones in each realisation, as has been highlighted in numerous
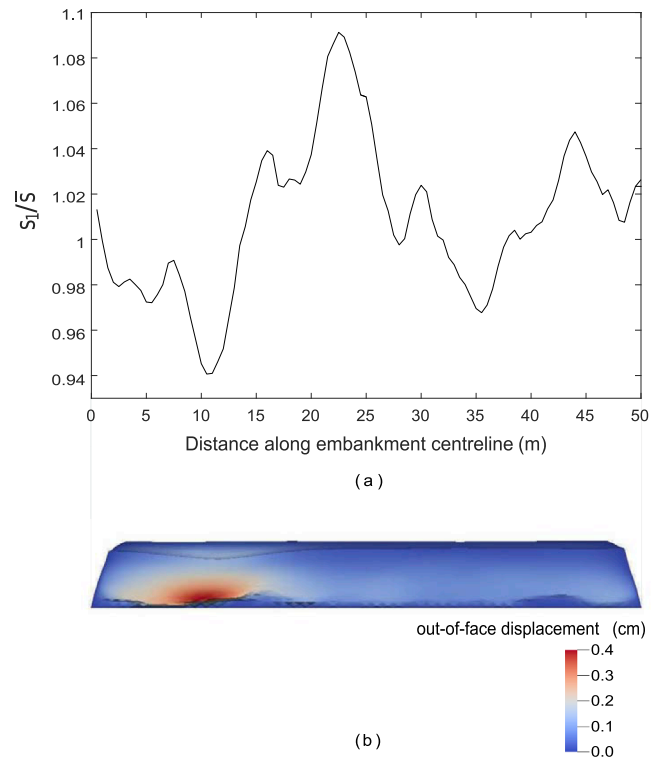
previous slope reliability studies (e.g., [4,6]). Similar findings have also been reported by Ching and Phoon [34] and Ching et al. [35], who showed that the mean shear strength over the failure surface is typically lower than $\bar{s}$ for various 2D boundary value problems. All these studies have highlighted the difference between spatial averaging over the whole domain and spatial averaging over an emergent slip surface, which is the solution of a boundary value problem over a spatially variable domain and hence changes from realisation to realisation.

This paper quantifies the difference between the two spatial averages and proposes a reduction factor (α) for the mean safety factor equal to the ratio of $\overline{s_b}$ to $\bar{s}$. This correction is not applied to the resistance from the end-sections, even though Vanmarcke's method also assumes $\overline{s_e} = \bar{s}$ in Eq. (4), as the vertical sides of the failure surface generally pass through a spatially more variable domain due to a relatively low value of the vertical scale of fluctuation compared to H [3]. Thus, the mean factor of safety in Eq. (15) changes to

$$\overline{F_b} = \overline{F}\left[\alpha + \frac{d}{b}\right]\beta \tag{16}$$

Fig. 6 shows the results for a typical RFEM realisation, illustrating that failure is often located around the point where the averaged shear strength per unit cross-section (s_1) is a minimum (in this case, at 10 m along the slope). This critical point is considered as the centre of the most-probable failure surface for the purpose of estimating α. The steps to compute α are:

- Generate 3D random fields of the shear strength parameters (e.g., using LAS).
- For each realisation:
  - Identify the critical cross-section, i.e., the one with the minimum s_1 (as in Fig. 6), along the embankment length;
  - Compute the average shear strength over the expected failure length (s_b), centred at the critical position.
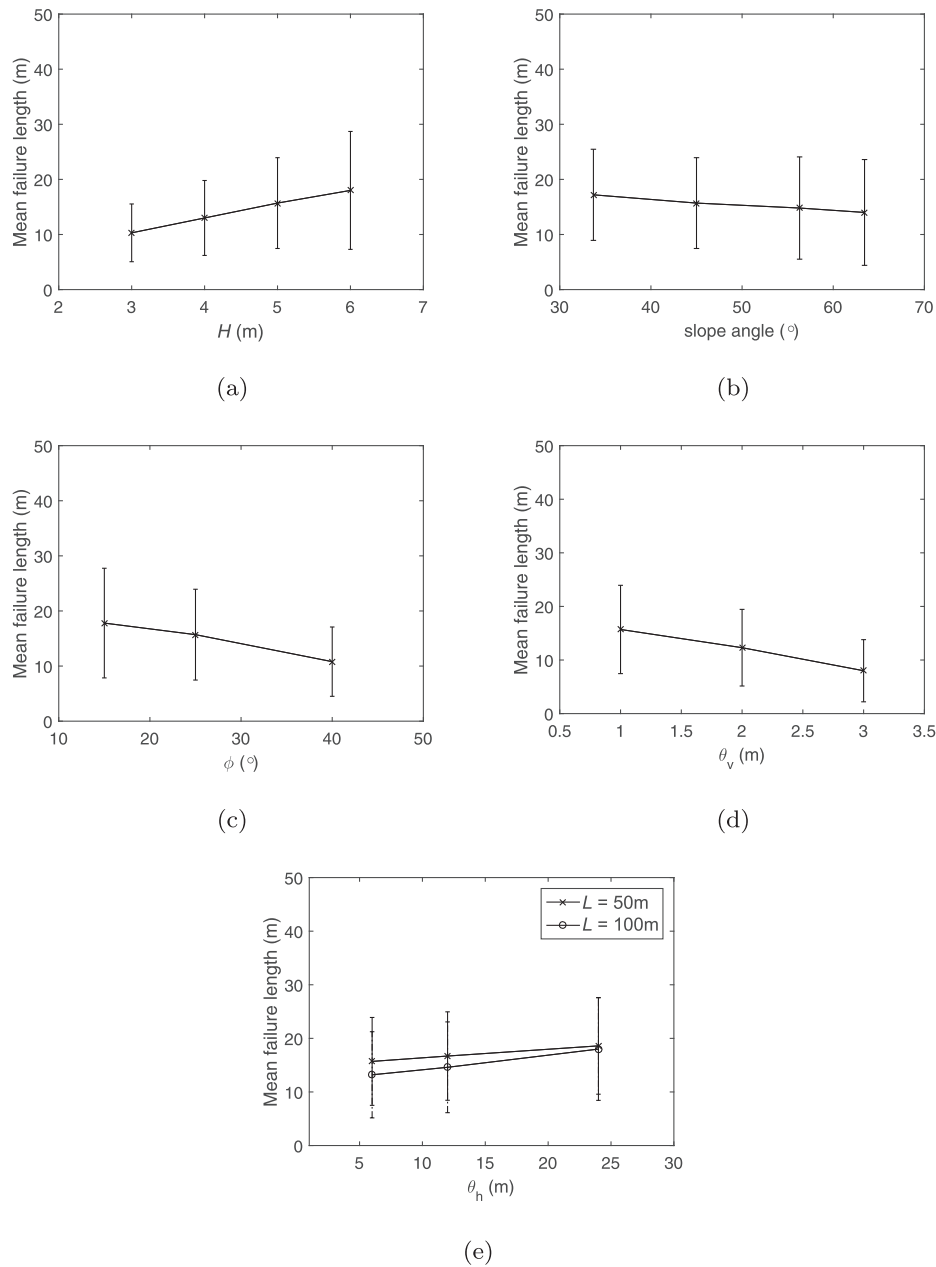- Repeat the above process for all realisations.

Fig. 7. Mean failure lengths with the associated one standard deviation error bar obtained by RFEM versus: (a) slope height (*H*); (b) slope angle; (c) friction angle (ϕ); (d) vertical scale of fluctuation (θ_v); (e) horizontal scale of fluctuation (θ_h).

- $\overline{s_b}$ = average of s_b over all the realisations.
- $\alpha = \overline{s_b}/\overline{s}$.

Since an actual slip surface is a function of the boundary value problem and spatial variability in each realisation, its shape and orientation cannot be determined without doing a finite element analysis. Therefore, the averaging of shear strength is carried out over a three dimensional domain (of dimensions comparable to the expected failure cross-section and length) that can encompass an emergent slip surface. Although this will tend to give an upper bound to the actual $\overline{s_b}$, due to the actual slip surface being attracted to the weaker zones, it nevertheless provides a reasonable first approximation.

5.3. Expected failure length

Since RFEM results indicate the influence of weak zones on the failure mechanism (cf. Calle [30], who suggested that the real failure, if

it occurs, coincides with the length of a potentially unstable zone), the averaging of shear strength needs to be carried out along this potential failure zone. However, the length of this potential failure does not necessarily coincide with the critical failure length predicted by Vanmarcke [25], since the latter does not take into account the influence of weak zones.

Hicks and Li [29] compared the failure lengths computed using RFEM, Vanmarcke's method and the "2.5D" method of Calle for very long slopes in cohesive soils. They showed that Calle's method and Vanmarcke's method underestimate the potential failure length at small θ_h. For very small θ_h relative to *H*, the failure length calculated by RFEM tends to be very long, extending over the entire length of the slope in each realisation. For larger θ_h, the mean RFEM failure length tends towards Calle's solution. Since neither of the two methods (Vanmarcke's method nor Calle's 2.5D method) predict the failure length accurately for all values of θ_h, it was proposed to use the mean failure length calculated by RFEM as the averaging length in the
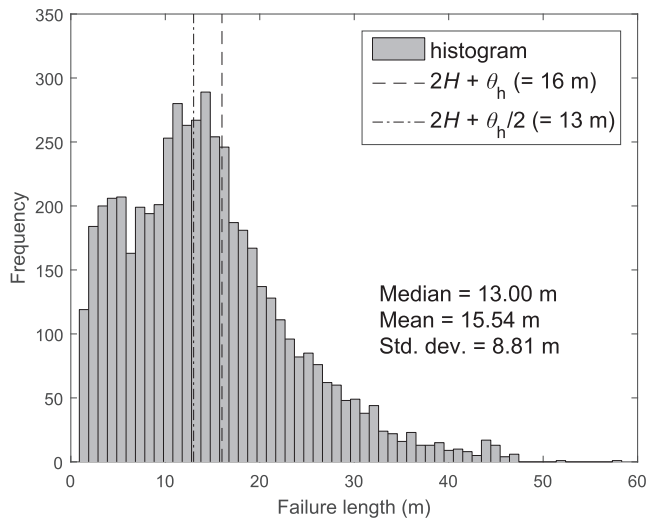
Fig. 8. Histogram of failure lengths obtained in each realisation of 3D RFEM analyses of a 5 m high slope for the various scenarios considered in Figs. 7(b)–(d).
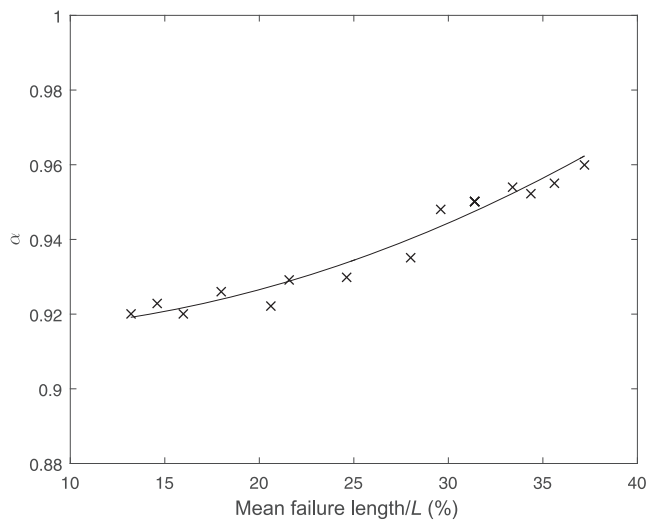

Fig. 9. α for all cases considered in Figs. 7(a)–(e).

modified Vanmarcke method (MVM). However, because the use of RFEM to determine the averaging length is computationally expensive, which rather defeats the purpose of using MVM, an approximate equation for the mean failure length (based on RFEM) is proposed in this paper.

Figs. 7(a)–(e) show the sensitivity of the mean failure length (computed using RFEM) to several parameters: H, slope angle, ϕ, θ_v, θ_h and slope length (L). Fig. 8 shows the histogram of failure lengths obtained from multiple 3D RFEM realisations of a 5 m high slope with $\theta_h = 6$ m, for the various values of slope angle, friction angle and θ_v considered in Figs. 7(b)–(d). Based on this sensitivity analysis,

Table 2
Table of recommended correction factor values.

Mean failure length/H	β	Mean failure length/L (%)	α
1–2	0.80–0.85	<15	0.920
2–3	0.85–0.89	15–22	0.920–0.930
3–5	0.89–0.92	22–28	0.930–0.940
5–20	0.92–0.97	28–37	0.940–0.965
>20	0.97–1.00	>37	0.965–1.000

Table 3
List of compared approaches.

Approach	Description
RFEM	Random finite element method
VM	Vanmarcke's method
MVM-1	MVM based on the mean failure length obtained by RFEM
MVM-2	MVM based on the failure length given by $2H + \theta_h/2$
MVM-3	MVM based on the failure length given by $2H + \theta_h$

Table 4
Mean failure lengths obtained by RFEM, corresponding correction factors and mean FS calculated by using MVM-1 for the base case.

θ_h (m)	Mean failure length (m)	β	α	Mean FS
1	37.0	0.940	1.000	1.408
6	15.7	0.881	0.950	1.375
12	16.7	0.882	0.954	1.369
24	18.6	0.895	0.960	1.377

the failure length is clearly a complex function of the soil spatial variability, as well as of the geometry of the boundary value problem. The median and mean of the histogram of failure lengths, obtained for the range of possible values of parameters considered, are approximately equal to $2H + \theta_h/2$ and $2H + \theta_h$, respectively (see Fig. 8), and are used here as approximate solutions instead of the complex function of failure length for intermediate values of θ_h (i.e., for $H < \theta_h < L/2$, as consistent with Mode 2 failures in Hicks and Spencer [4]).

5.4. Recommended values for correction factors

Based on the RFEM computations of the mean failure length, Fig. 9 shows the values of the correction factor α for the range of parameter values considered in Figs. 7(a)–(e). Since α is calculated as the ratio of the averaged shear strength over a failed segment to the averaged shear strength over the entire slope, the failure length is normalised by L in Fig. 9. The value of α approaches unity for very long failures relative to L, whereas for intermediate failure lengths relative to L, α lies between 0.92 and 0.96. The recommended values of β and α for a range of values of the failure length are summarised in Table 2 (based on Figs. 5 and 9, respectively). Note that the β values reported in Table 2 correspond to a soil with a friction angle of 25°. Slight variations in the value of β, with respect to those reported in Table 2, are expected for cases with higher or lower values of friction angle (see Fig. 5).

## 6. Methodology and analysis

The steps followed to compute the mean FS (and standard deviation of FS) of slopes with the proposed modified Vanmarcke method are:

- Calculate the 2D FS based only on the mean values of the soil parameters.
- Calculate the effective width d of the end-sections using Eq. (8).
- Calculate the approximate failure length using either $2H + \theta_h/2$ or $2H + \theta_h$.
- Obtain β from Fig. 5 or use the recommended values in Table 2.
- Obtain α from Fig. 9 or use the recommended values in Table 2.
- Calculate the mean FS using Eq. (16).
- Calculate the standard deviation of FS using Eq. (12).

In order to test the methodology the 5 approaches listed in Table 3 have been compared for a base case problem. Note that approach MVM-1, which uses the mean failure length obtained by RFEM analysis, has been considered in order to check which one of the two simpler expressions for the failure length is a good approximation.
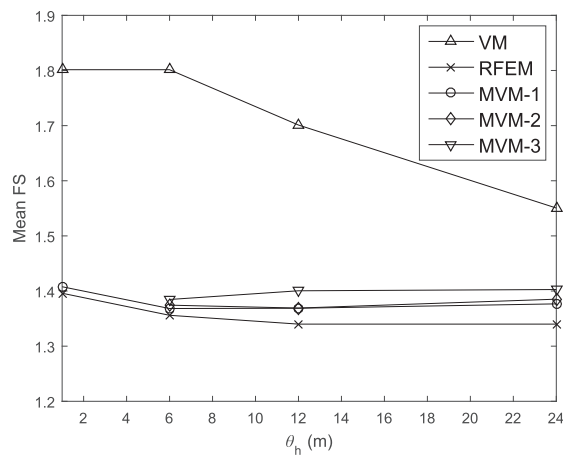
(a) Mean 3D FS as a fuction of θ_h
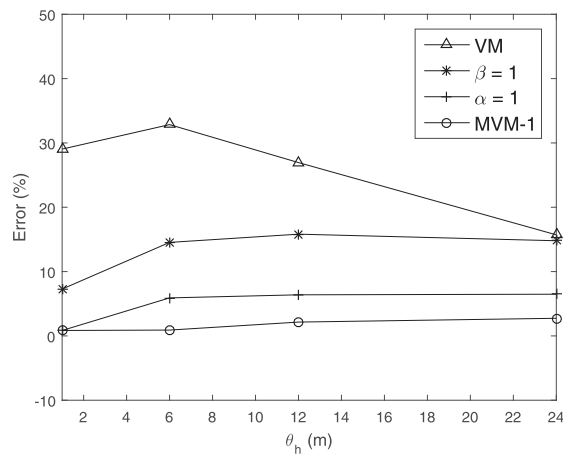
(b) Error in mean 3D FS by VM and MVM-1 with respect to mean 3D FS by RFEM

Fig. 10. Comparison of mean 3D FS by the different methods and relative influence of correction factors for the base case.
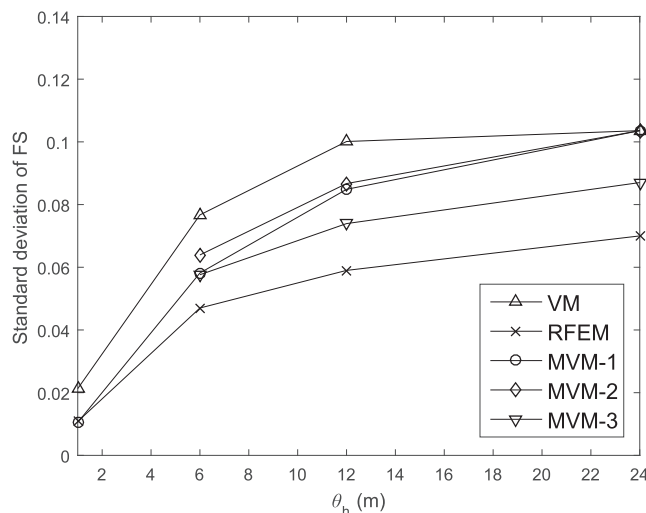
Fig. 11. Comparison of standard deviation of 3D FS by the different methods for the base case.

A 50 m long slope, again with the cross-sectional geometry shown in Fig. 1, the soil parameters listed in Table 1 and a vertical scale of fluctuation of 1 m has been considered. The mean failure lengths obtained by RFEM for different values of θ_h and the corresponding correction factors are summarised in Table 4 and represent the base case.
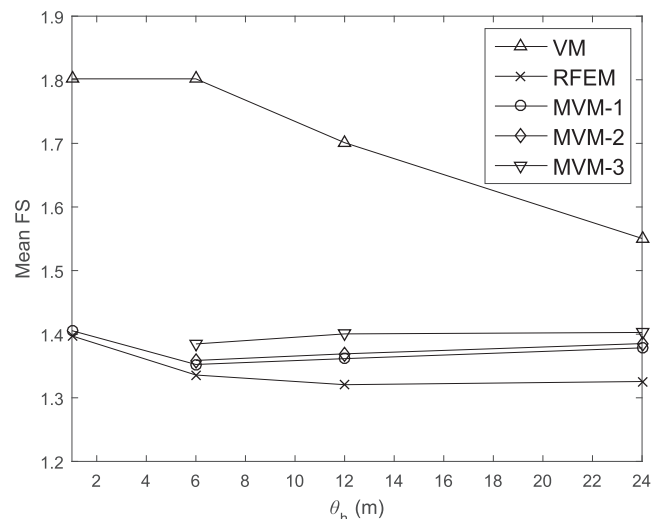
(a) $\theta_v = 2\,\text{m}$
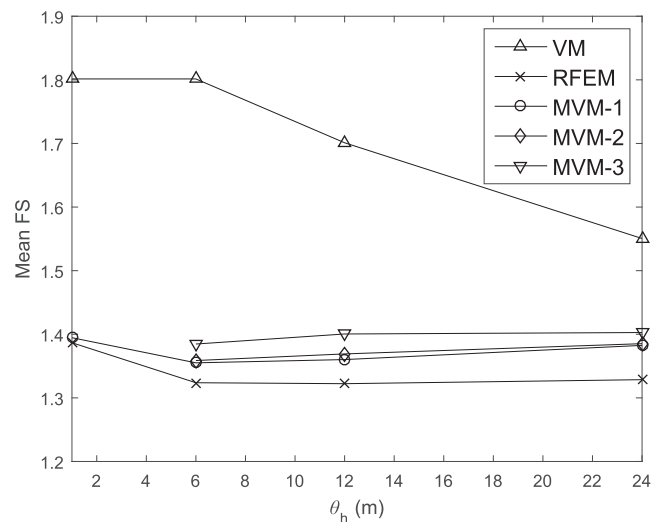
(b) $L = 100\,\text{m}$

Fig. 12. Comparison of mean 3D FS by RFEM, VM and MVM for two additional cases.

The mean FS obtained by using the different methods and the relative influence of each correction factor (in MVM-1) towards improving the mean FS for the base case are plotted in Fig. 10. At very small θ_h the major improvement is due to considering the correct failure length and correcting for the overestimated contribution to resistance from the end-sections. For intermediate values of θ_h, each correction factor has a considerable influence on the results, although α has relatively lower importance than the other two factors for this particular example. The small remaining error in the MVM-1 analysis may be attributed to an overestimated α, due to the averaging of shear strength being carried out over entire cross-sections of the slope segments, since the exact shape of the failure surface is not known a priori.

Fig. 11 compares the standard deviation of the 3D FS obtained by the different methods. The standard deviation has not improved as significantly as the mean, but it remains above that obtained using RFEM and is thus conservative. The difference between the VM and MVM results is mainly due to the different failure lengths used in the two methods. The main difference between the MVM and RFEM results may be attributed to the approximate form of the variance reduction factor used in Vanmarcke's method, compared to the variance reduction factor derived from the covariance function used in the RFEM model in
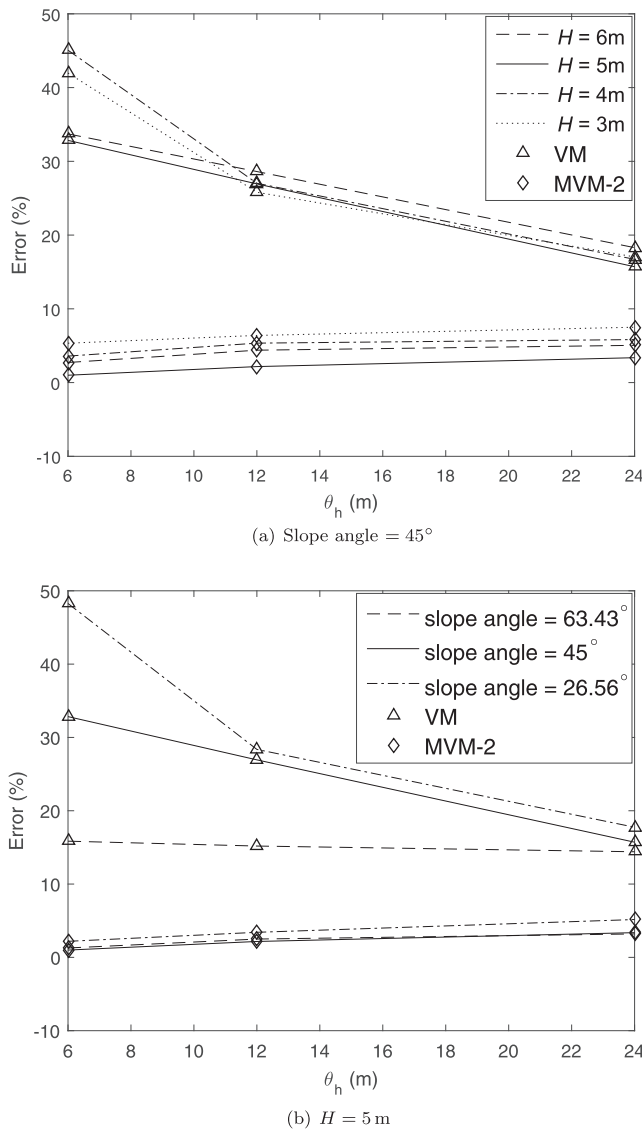
(a) Slope angle = 45°

(b) $H = 5$ m

Fig. 13. Error in mean 3D FS by VM and MVM-2 (relative to RFEM) for different cross-sectional geometries.

failure length calculated by $2H + \theta_h/2$, are in good agreement with the RFEM mean FS for all cases considered. Thus the proposed simplified expression ($b = 2H + \theta_h/2$) for the failure length seems a good approximation, although good results have also been obtained using $b = 2H + \theta_h$. Note that Hicks and Li [29] conducted 3D RFEM analysis on much longer slopes with undrained shear strength parameters, where the boundary effects have negligible influence on the calculated failure length and FS. Their study also implied a mean discrete failure length approximately equal to $2H + \theta_h/2$ (see [29]) and thus reinforces the findings in this paper.

Figs. 10–12 are based on the 3D FS computed for slopes with the specific cross-sectional geometry shown in Fig. 1. However, the influence of different cross-sectional geometry parameters, such as H and slope angle, on the expected failure length (Figs. 7(a)–(b) and Fig. 8) were taken into account in deriving the correction factors for the modified Vanmarcke method, implying that the applicability of the proposed method is not restricted to the one cross-section. Hence, in order to demonstrate its wider applicability, additional cases of slopes with different cross-sectional geometries (H and slope angle) have been considered. These further analyses have been based on slopes that are 50 m long in the third dimension, the soil parameters listed in Table 1 and a vertical scale of fluctuation of 1 m. The results, expressed in terms of percentage error in the mean FS computed by VM and MVM-2 relative to the mean FS computed by RFEM, are plotted in Fig. 13, and the failure lengths obtained by the various approaches are listed in Tables 5 and 6. Fig. 13 shows that the mean FS computed by MVM-2 has an error <8% (relative to the mean FS computed by RFEM) and is substantially better than the mean FS computed by VM (with an error of approximately 15–50%, and a tendency for larger errors at lower θ_h) for the range of parameters considered. This improvement is partly driven by the improved estimates of the failure lengths shown in Tables 5 and 6. Note that the relatively higher error in the mean FS computed by VM at $\theta_h = 6$ m, for slopes with $H = 3$ m, $H = 4$ m and slope angle = 26.56°, is due to the very short failure length predicted by VM (see Tables 5 and 6) in these cases.

The proposed method has been shown to work well for all test cases considered in this paper. However, a few limitations of the proposed method, which are beyond the scope of this paper, are that it cannot be applied to slopes in which the failure surface passes through multiple soil layers, nor to slopes with cross-sections or soil layer depths varying along the embankment length, and nor to slopes made up of soils with multiple scales of fluctuation of the inherent shear strength.

7. Conclusions

A modified semi-analytical method for slope reliability has been proposed based on Vanmarcke's [25] method. A comprehensive numerical investigation identified three significant areas which required improvement. These were corrected by an alternative relationship for the expected failure length (equal to $2H + \theta_h/2$ for intermediate values of θ_h) and a modified equation (Eq. (16)) for the mean FS that utilises two correction factors, α and β. Calibration curves for the correction factors are provided and recommended values for these factors are summarised in Table 2. These

this paper. Note that in Fig. 10(a), and Fig. 11, the mean and standard deviation of FS are not calculated for very small values of θ_h ($<H$) by MVM-2 and MVM-3, since the approximate equation for the failure length does not hold true for this range of θ_h.

Two additional cases with the same cross-sectional geometry have been considered: one with a higher value of θ_v and the other with a longer slope length ($L = 100$ m). The mean FS obtained by using the different methods considered in this paper are plotted in Fig. 12. Overall, Figs. 10 and 12 show that the mean FS obtained by MVM, based on the mean failure length obtained by RFEM, or based on the

Table 5
Failure lengths obtained by VM and MVM-2, and mean failure lengths obtained by RFEM, for slopes of different height and slope angle = 45°.

θ_h (m)	$H = 3$ m				$H = 4$ m				$H = 5$ m				$H = 6$ m			
	$\overline{F}$	Failure length (m)			$\overline{F}$	Failure length (m)			$\overline{F}$	Failure length (m)			$\overline{F}$	Failure length (m)		
		VM	MVM-2	RFEM		VM	MVM-2	RFEM		VM	MVM-2	RFEM		VM	MVM-2	RFEM
6	1.92	6.0	9.0	12.5	1.60	6.1	11.0	14.4	1.40	9.0	13.0	15.7	1.29	13.6	15.0	15.9
12	1.92	12.0	12.0	14.3	1.60	12.0	14.0	15.8	1.40	12.0	16.0	16.7	1.29	13.6	18.0	16.8
24	1.92	24.0	18.0	18.0	1.60	24.0	20.0	18.2	1.40	24.0	22.0	18.6	1.29	24.0	24.0	21.1

Table 6
Failure lengths obtained by VM and MVM-2, and mean failure lengths obtained by RFEM, for slopes of different slope angle and $H = 5$ m.

θ_h (m)	Slope angle = 26.56°				Slope angle = 45°				Slope angle = 63.43°			
	$\overline{F}$	Failure length (m)			$\overline{F}$	Failure length (m)			$\overline{F}$	Failure length (m)		
		VM	MVM-2	RFEM		VM	MVM-2	RFEM		VM	MVM-2	RFEM
6	2.08	6.0	13.0	16.7	1.40	9.0	13.0	15.7	1.10	27.4	13.0	12.7
12	2.08	12.0	16.0	17.4	1.40	12.0	16.0	16.7	1.10	27.4	16.0	14.2
24	2.08	24.0	22.0	20.2	1.40	24.0	22.0	18.6	1.10	27.4	22.0	18.1

suggest that, for very long embankments, $\alpha \approx 0.92$ and $0.85 \leqslant \beta \leqslant 0.92$ may be reasonable first approximations. The mean FS obtained by using the modified method was in good agreement with the mean FS obtained by RFEM for all cases considered in this paper.

Acknowledgements

References

[1] Phoon K-K, Kulhawy FH. Characterization of geotechnical variability. Can Geotech J 1999;36(4):612–24.

[2] Jaksa M, Kaggwa W, Brooker P. Experimental evaluation of the scale of fluctuation of a stiff clay. In: Proceedings of 8th International Conference on the Application of Statistics and Probability in Civil Engineering, Sydney; 1999. p. 415–422.

[3] de Gast T, Vardon PJ, Hicks MA. Estimating spatial correlations under man-made structures on soft soils. In: Proceedings of 6th International Symposium on Geotechnical Safety and Risk, Colorado; 2017. p. 382–389.

[4] Hicks MA, Spencer WA. Influence of heterogeneity on the reliability and failure of a long 3D slope. Comput Geotech 2010;37(7–8):948–55.

[5] Hicks MA, Nuttall JD, Chen J. Influence of heterogeneity on 3D slope reliability and failure consequence. Comput Geotech 2014;61:198–208.

[6] Hicks MA, Samy K. Influence of heterogeneity on undrained clay slope stability. Q J Eng Geol Hydrogeol 2002;35(1):41–9.

[7] Hicks MA, Onisiphorou C. Stochastic evaluation of static liquefaction in a predominantly dilative sand fill. Géotechnique 2005;55:123–33.

[8] Cho SE. Effects of spatial variability of soil properties on slope stability. Eng Geol 2007;92(3–4):97–109.

[9] Griffiths DV, Huang J, Fenton GA. Influence of spatial variability on slope reliability using 2-D random fields. J Geotech Geoenviron Eng 2009;135:1367–78.

[10] Baecher GB, Christian JT. Reliability and statistics in geotechnical engineering. John Wiley & Sons; 2003.

[11] Hasofer AM, Lind MC. An exact and invariant first order reliability format. J Eng Mech 1974;100:111–21.

[12] Sudret B, Der Kiureghian A. Stochastic finite element methods and reliability: a state-of-the-art report. Department of Civil and Environmental Engineering, University of California Berkeley; 2000.

[13] Rosenblueth E. Two-point estimates in probabilities. Appl Math Model 1981;5(5):329–35.

[14] Li D-Q, Jiang S-H, Cao Z-J, Zhou W, Zhou C-B, Zhang L-M. A multiple response-surface method for slope reliability analysis considering spatial variability of soil properties. Eng Geol 2015;187:60–72.

[15] Jiang S-H, Li D-Q, Cao Z-J, Zhou C-B, Phoon K-K. Efficient system reliability analysis of slope stability in spatially variable soils using Monte Carlo simulation. J Geotech Geoenviron Eng 2015;141(2):1–13.

[16] Fenton GA, Griffiths DV. Risk assessment in geotechnical engineering Vol. 461. Wiley Online Library; 2008.

[17] Hicks MA, Samy K. Stochastic evaluation of heterogeneous slope stability. Ital Geotech J 2004;38(2):54–66.

[18] Lloret-Cabot M, Hicks MA, van den Eijnden AP. Investigation of the reduction in uncertainty due to soil variability when conditioning a random field using Kriging. Géotechnique Lett 2012;2(3):123–7.

[19] Li Y, Hicks MA, Vardon PJ. Uncertainty reduction and sampling efficiency in slope designs using 3D conditional random fields. Comput Geotech 2016;79:159–72.

[20] Arnold P, Hicks MA. A stochastic approach to rainfall-induced slope failure. In: Proceedings of 3rd International Symposium on Safety and Risk, Munich; 2011. p. 107–115.

[21] Vardon PJ, Liu K, Hicks MA. Reduction of slope stability uncertainty based on hydraulic measurement via inverse analysis. Georisk: Assess Manage Risk Eng Syst Geohazards 2016;10(3):223–40.

[22] Spencer WA, Hicks MA. A 3D finite element study of slope reliability. In: Proceedings of 10th International Symposium on Numerical Models in Geomechanics, Rhodes; 2007. p. 539–543.

[23] Hicks MA, Chen J, Spencer WA. Influence of spatial variability on 3D slope failures. In: Proceedings of 6th International Conference on Computer Simulation in Risk Analysis and Hazard Mitigation, Kefalonia; 2008. p. 335–342.

[24] Huang J, Lyamin AV, Griffiths DV, Krabbenhoft K, Sloan S. Quantitative risk assessment of landslide by limit analysis and random fields. Comput Geotech 2013;53:60–7.

[25] Vanmarcke EH. Reliability of earth slopes. J Geotech Eng Div 1977;103(11):1247–65.

[26] Vanmarcke EH. Probabilistic stability analysis of earth slopes. Eng Geol 1980;16(1-2):29–50.

[27] Li Y, Hicks MA, Nuttall JD. Comparative analyses of slope reliability in 3D. Eng Geol 2015;196:12–23.

[28] Varkey D, Hicks MA, Vardon PJ. Influence of spatial variability of shear strength parameters on 3D slope reliability and comparison of analysis methods. In: Proceedings of 6th International Symposium on Geotechnical Safety and Risk, Colorado; 2017. p. 400–409.

[29] Hicks MA, Li Y. Influence of length effect on embankment slope reliability in 3D. Int J Numer Anal Meth Geomech 2018;42:891–915.

[30] Calle E. Probabilistic analysis of stability of earth slopes. In: Proceedings of 11th International Conference on Soil Mechanics and Foundation Engineering, California; 1985. p. 809–812.

[31] Fenton GA, Vanmarcke EH. Simulation of random fields via local average subdivision. J Eng Mech 1990;116(8):1733–49.

[32] Spencer WA. Parallel stochastic and finite element modelling of clay slope stability in 3D. Ph.D. thesis. University of Manchester, UK; 2007.

[33] Cherubini C. Reliability evaluation of shallow foundation bearing capacity on c', ϕ' soils. Can Geotech J 2000;37(1):264–9.

[34] Ching J, Phoon K-K. Mobilized shear strength of spatially variable soils under simple stress states. Struct Saf 2013;41:20–8.

[35] Ching J, Hu Y-G, Phoon K-K. On characterizing spatially variable soil shear strength using spatial average. Probab Eng Mech 2016;45:31–43.